eng

MDPI

Article

Transforming Denim Waste: Super Glue-Enhanced Composite Materials

Christina Gioti [1,*], Dimitrios Moschovas [1], Apostolos Avgeropoulos [1], Constantinos E. Salmas [1], Simeon Agathopoulos [1], Athanasios B. Bourlinos [2] and Michael A. Karakassides [1,*]

[1] Department of Materials Science and Engineering, University of Ioannina, GR-45110 Ioannina, Greece; dmoschov@uoi.gr (D.M.); aavger@uoi.gr (A.A.); ksalmas@uoi.gr (C.E.S.); sagat@uoi.gr (S.A.)
[2] Physics Department, University of Ioannina, GR-45110 Ioannina, Greece; bourlino@uoi.gr
* Correspondence: christina.gioti@uoi.gr (C.G.); mkarakas@uoi.gr (M.A.K.); Tel.: +30-26510-07350 (C.G.); +30-26510-07276 (M.A.K.)

Abstract

The present study demonstrated the fabrication of a sustainable, high-performance composite by upcycling waste denim fabric within a cyanoacrylate matrix reinforced with B_4C micro-particles (4, 7, and 10 wt%). XRD and SEM analyses confirmed the successful integration of the ceramic filler and effective fiber encapsulation, with particle agglomeration identified at 10 wt% loading. The 7 wt% B_4C composition exhibited the highest static mechanical performance, with a tensile strength of ~20.3 ± 1.3 MPa and Young's modulus of 1.17 GPa—improvements of ~22.8% and ~41% over the unreinforced denim–cyanoacrylate composite—while at 10 wt% B_4C the ultimate tensile strength declined below the unreinforced baseline and the Young's modulus reverted to a comparable value, likely reflecting agglomeration-induced stress concentration as a major contributing factor. Under dynamic impact loading, the peak contact force increased monotonically from 0.34 kN to 1.31 kN with increasing B_4C content yet remained well below the thresholds specified by international impact protection standard thresholds across all compositions. This divergence between static and dynamic responses indicates that the increase in contact force with B_4C content reflects progressive stiffening and more direct load transfer rather than improved energy attenuation, whereas tensile performance depends critically on dispersion quality and fiber–matrix adhesion. Surface wettability analysis showed a marked increase in hydrophobicity, with the water contact angle rising from 105 ± 4° to 133 ± 4° (for the DSGB-7 wt% composite), consistent with a Cassie–Baxter wetting regime. These preliminary results suggest that B_4C-reinforced waste denim–cyanoacrylate composites merit further investigation as candidate materials platform for protective textile applications, pending validation through larger-scale, standardized testing.

Keywords: waste denim; cyanoacrylate; super-glue; textile composite; boron carbide; impact; tensile properties; hydrophobicity; upcycling

Check for updates

Academic Editor: Ruochen Liu

Received: 4 July 2026
Revised: 4 August 2026
Accepted: 5 August 2026
Published: 7 August 2026

Copyright: © 2026 by the authors. Licensee MDPI, Basel, Switzerland. This article is an open access article distributed under the terms and conditions of the Creative Commons Attribution (CC BY) license.

1. Introduction

Jeans are among the most widely worn garments today. Their popularity has been driven by the rise in casual fashion and the availability of affordable, durable denim. The global denim market has seen steady growth in recent years and is projected to exceed USD 100 billion by 2030, with an estimated production of nearly 3.5 billion pairs of jeans annually [1,2]. This massive production and consumption result in significant denim

waste at the end of the garments' service life. Each year, approximately 2.16 million tons of used jeans are discarded globally, typically ending up in landfills or incinerators [3]. Landfilled denim contributes to methane emissions from decomposing cotton [4] and can contaminate soil and water due to textile effluents containing indigo dye [5,6]. Meanwhile, incineration releases carbon dioxide and other greenhouse gases from burning organic material [7]. Given the large volume of discarded jeans, recycling is essential to mitigate the environmental impact of denim waste.

The main approaches to recycling include mechanical recycling, upcycling, chemical recycling, downcycling, and closed-loop recycling [8–13]. Mechanical recycling converts waste denim by shredding or unraveling it into fibers, which are re-spun into yarns for recycled denim fabrics or other textiles, often using uniform manufacturing scraps for weft yarns, while upcycling creatively transforms worn jeans into valuable products like insulation, bags, or home furnishings. Chemical recycling employs advanced technologies to break down cotton into glucose and isolate polyester for reuse, enabling sustainable material recovery. Downcycling repurposes denim into lower-value items like mattress stuffing or construction composites, such as denim–polypropylene blends, while closed-loop recycling collects post-consumer jeans to produce high-quality recycled denim fabrics, fostering a circular system that minimizes waste and promotes sustainability.

Recycled denim fabric also demonstrates considerable promise as a reinforcement material in polymer composites [14–23]. Previous studies have incorporated denim blended with various everyday polymers (polyethylene, polypropylene, epoxy, polyurethane) to fabricate reinforced composites; for example, one study explored the fabrication of composites using epoxy resin reinforced with recycled cotton textile waste [21]. In this research, denim fabric was shredded and used as a reinforcing agent, comprising roughly 30% of the composite material. The resulting epoxy-based composite exhibited notable enhancements in mechanical performance, including a twofold increase in both tensile strength (from 0.09 to 0.16 MPa) and Young's modulus (from 0.5 to 1.2 MPa) compared to unreinforced epoxy. Tensile testing indicated strong interfacial bonding between the epoxy matrix and the denim fibers, likely due to the presence of fibrils and microfibrils generated during the shredding process. These findings support the potential use of recycled denim–epoxy composites in applications such as fashion items or structural components. In a separate study, textile waste from knitted garments, including denim, was integrated into polyurethane foam to develop composite materials [22]. These composites contained up to 40% textile waste and demonstrated improved mechanical characteristics along with enhanced acoustic properties. Specifically, the inclusion of denim fabric led to a noise reduction coefficient (NRC) that was twice that of pure polyurethane foam, indicating their suitability for structural uses such as automotive parts or acoustic insulation panels.

Although no existing research has specifically explored the use of superglue (cyanoacrylate) [24,25] in combination with denim fabric for polymer composites, this pairing offers several promising advantages, including fast fabrication, strong initial adhesion, lightweight structural reinforcement, water resistance, and cost-efficiency. Cyanoacrylate's rapid curing—ranging from seconds to minutes—enables much quicker bonding compared to slower-curing resins like epoxy or polyurethane, which may take hours or even days to cure. Its low viscosity allows it to penetrate deeply into the cotton fibers of denim, resulting in a strong and uniform bond throughout the material. This high penetration ability enhances adhesion and contributes to the formation of a tightly bonded composite. Additionally, superglue can rigidify denim without significantly increasing its weight, offering a lightweight yet stiff material. Once cured, it forms a water-resistant barrier that may improve the fabric's water repellency. Lastly, the combination of inexpensive, readily available superglue and recycled denim makes this approach economically viable.

In the present study, waste denim–cyanoacrylate composites containing approximately 44 wt% cyanoacrylate polymer (determined for the unreinforced denim–cyanoacrylate reference composite; see Section 2.2)—the minimum required to effectively wet and bind the denim fabric—reinforced with boron carbide (B_4C) micro-particles at concentrations of 4, 7, and 10 wt%. Boron carbide was specifically selected over more conventional ceramic fillers such as Al_2O_3, SiC, or SiO_2 due to its unique combination of exceptional hardness (Mohs ~9.5) and low density (2.52 g/cm^3), which together make it the established material of choice in high-performance ceramic armor applications [26–28]. While B_4C is acknowledged to be a relatively expensive technical ceramic, its use at low filler loadings (4–10 wt%) limits the absolute material cost per composite, and the present study is primarily intended as a proof-of-concept investigation. The substitution of B_4C with lower-cost ceramic alternatives remains an important direction for future work, making it an appropriate candidate for mechanical reinforcement applications [29]. The investigation aims to evaluate the effect of B_4C filler concentration on the structural, morphological, surface wettability, and mechanical properties of the resulting composites, with particular focus on identifying the threshold of optimal particle dispersion and its influence on both static and dynamic mechanical response. The developed composites are assessed for their potential as candidate materials for personal protective equipment (PPE) applications, offering a promising and eco-friendly route for the upcycling of textile waste into value-added technical materials.

2. Materials and Methods

2.1. Materials

The fabrication of the superglue-enhanced composites utilized repurposed commercial waste blue denim fabric as the primary substrate (hereafter referred to simply as "denim (D)". The denim substrate consisted of heavily worn, end-of-life waste fabric purchased from the Greek market, representing a real post-consumer textile waste stream. Extensive prior use and washing cycles are expected to have substantially degraded any residual elastane and indigo dye content, rendering the substrate predominantly cellulosic in character. Since recycled denim may originate from different sources, variations in fiber composition and degree of wear may influence composite performance. A systematic evaluation of these parameters would provide further insight into the optimization and standardization of the proposed upcycling approach. Furthermore, a commercial-grade cyanoacrylate adhesive, commonly referred to as "super glue", served as the matrix phase. To enhance the composite properties, boron carbide (B_4C) was incorporated as a particulate filler, sourced from Sigma-Aldrich, St. Louis, MO, USA (powder form, particle size < 10 μm, 98% purity, product #378119-50G).

2.2. Preparation of Denim–Cyanoacrylate (DSG) Composites

For the preparation of the composites, the waste denim fabric was cut into uniform dimensions of 5 × 5 cm and 10 × 1.5 cm. The polymer matrix was formulated by diluting commercial cyanoacrylate UHU BISON-super glue with a minimal volume of acetone to reduce viscosity and facilitate uniform application. The mixture was applied to the dual-layer denim assembly within 1–2 min using a manual brushing technique, with fabric edges secured by adhesive tape to maintain dimensional stability and prevent wrinkling during curing. No separate acetone evaporation step was required, as polymerization initiated immediately upon contact with the fabric surface. The assembly was impregnated from both sides to ensure uniform through-thickness matrix saturation. Specimens were cured at room temperature for a minimum of two weeks prior to testing. The thickness of the raw denim sheet was measured as 0.69 ± 0.03 mm, while the final composite thicknesses were 2.15 mm for the neat denim–cyanoacrylate composite (DSG).

These composite samples will hereafter be referred to as "DSG" samples. To quantify the degree of cyanoacrylate uptake, all specimens were weighed prior to and following adhesive impregnation using a precision analytical balance. The results revealed an average mass increase of approximately 80 wt% relative to the dry denim substrate, confirming that the adhesive penetrated extensively into the fibrous network and was effectively retained within the composite structure upon curing. Formal confirmation of complete solvent removal was not performed in the present study and is identified as a direction for future work. This value, and the corresponding ~44 wt% cyanoacrylate mass fraction reported in the manuscript, refer specifically to the unreinforced denim–cyanoacrylate (DSG) composite. For the B_4C-loaded (DSGB) compositions, the cyanoacrylate mass fraction was not independently determined following B_4C incorporation. Since the total composite mass of the DSGB specimens includes the additional B_4C content, the relative cyanoacrylate mass fraction is expected to be lower than that of the DSG reference, assuming comparable adhesive uptake during fabrication.

2.3. Preparation of B_4C-Reinforced Denim–Cyanoacrylate (DSGB) Composites

For the preparation of the reinforced composite specimens, B_4C was incorporated into the denim layers at three distinct concentrations: 4, 7, and 10 wt%. The measured powder was suspended in a minimal volume of ethanol to create a workable slurry, in which the denim samples were immersed. This allowed the B_4C particles to be effectively absorbed into the fabric's fibrous structure. The samples were then dried in an oven at 70 °C for 1 h to ensure complete evaporation of ethanol prior to cyanoacrylate application. The B_4C mass content was controlled gravimetrically: the exact mass of B_4C powder was weighed prior to slurry preparation, and each specimen was re-weighed following oven drying (70 °C, 1 h) to confirm the mass of ceramic filler retained within the fabric structure. The target concentrations (4, 7, and 10 wt%) were calculated relative to the total composite mass and verified for each specimen using a precision analytical balance. To form the composite, two fabric sheets were stacked to create a dual-layer structure and impregnated from the top side with the cyanoacrylate adhesive. The adhesive successfully penetrated the first layer and diffused into the second, effectively wetting the interface between them. The assembly was then inverted, and the process was repeated on the reverse side to ensure complete and uniform saturation of the matrix. To ensure statistical reliability and reproducibility, three distinct samples were fabricated for each experimental composition. The final composite thickness, measured using a digital caliper at multiple positions, was: DSGB-4 wt%: 2.06 ± 0.10 mm; DSGB-7 wt%: 2.04 ± 0.04 mm; DSGB-10 wt%: 2.50 mm. Due to the instrument's precision limit (0.1 mm), localized thickness variations below this threshold resulted in identical rounded readouts for certain specimens, yielding average thickness values with an artificially negligible standard deviation. For compositions in which repeated thickness measurements yielded identical readings within the practical resolution of the digital caliper, only the average thickness value is reported. These composite samples will hereafter be referred to as "DSGB-x%" samples, with the value in parentheses indicating the wt% B_4C content. It is noted that the ~44 wt% cyanoacrylate mass fraction reported for the DSG reference composite (Section 2.2) was not independently re-verified for the DSGB compositions following B_4C incorporation.

2.4. Surface Wettability and Contact Angle Characterization

The wetting properties of the coated surfaces were investigated using the OCA-25 contact angle measuring device from DataPhysics Instruments GmbH (Filderstadt, Germany), controlled by the SCA-20 software (version 4.5.0, DataPhysics Instruments GmbH) The drop method was employed for static contact angle measurements and distilled deionized

water droplets of 4 µL were placed onto the surfaces at a rate of 0.5 µL/s under ambient conditions. The final contact angle was calculated as the average of at least five water droplets placed at different positions on the surface. Measurements were repeated on five independently prepared coated surfaces to assess the repeatability. The errors reported correspond to the standard deviation of the measurements.

2.5. X-Ray Diffraction Measurements

The crystalline structure and phase composition of the fabricated composites and raw materials were analyzed via X-ray diffraction (XRD) using a Rigaku MiniFlex benchtop diffractometer (Rigaku Corporation, Tokyo, Japan). The instrument operated with Cu Kα radiation (λ = 1.5418 Å) at an accelerating voltage of 40 kV and a current of 15 mA. The powder samples and composite sections were scanned over a 2θ range from 10° to 80° employing a step size of 0.01° (2θ) and a scanning speed of 5°/min per minute. Prior to analysis, the samples were mounted on standard glass holders, ensuring a flat surface for optimal diffraction. Phase identification was performed by comparing the resulting diffractograms with reference patterns from the Crystallography Open Database (COD).

2.6. Drop-Weight Impact Testing

The damage resistance of the DSGB composites was evaluated through drop-weight impact testing in accordance with ASTM D7136/D7136M [30], with specimen dimensions adapted to 5 × 5 cm to accommodate the available sample size. Low-velocity impact testing was performed using an Instron Ceast 9340 drop tower (Instron CEAST Division, Torino, Italy) equipped with a 45 kN load cell integrated into the impactor (tup), which recorded the impact contact force during testing. Specimens were centered over a high-strength steel support fixture with a rectangular cutout, ensuring consistent boundary conditions across all tests. A hemispherical striker, which was 16 mm in diameter and 2.5 kg in mass, was released from a predetermined height to deliver a specific impact energy to the center of each specimen. Two impact energy levels, 2 J and 10 J, were selected to evaluate the composite response under both low- and high-severity impact conditions. Preliminary impact tests were conducted at 2 J; however, no visible damage was observed at this energy level for any composition, confirming the high impact resistance of the fabricated composites. All quantitative results reported herein therefore correspond to the 10 J impact energy level, which was selected as the reference condition for comparative evaluation across all compositions. The drop tower was equipped with an anti-rebound mechanism to prevent secondary impacts that could otherwise compromise the analysis of the primary damage event. Following each impact event, specimens were visually inspected for surface indentation, fiber breakage, and delamination. For each composition, three specimens were tested per impact energy level, and the maximum impact load (kN) and absorbed energy (J) were recorded to characterize the toughening effect of B_4C reinforcement within the denim–polymeric matrix. The absorbed energy was calculated from the area under the load–displacement curve.

2.7. Tensile Properties Characterization

The tensile properties of the DSG and DSGB specimens were evaluated using an Autograph AGS-H testing machine (Shimadzu Corporation, Kyoto, Japan). Prior to testing, all specimens were conditioned at standard atmospheric conditions (65 ± 2% RH, 21 ± 1 °C) according to ASTM D 1776 and measured according to related test standards [31]. The tests were conducted at a constant crosshead speed of 1.5 mm/min until specimen fracture occurred. All specimens were cut parallel to the warp direction of the denim fabric. Tensile tests were performed with a gauge length of approximately 80 mm, with specimens clamped directly in the machine grips. The cross-sectional area was calculated as

width × thickness, using mean values from five geometric measurements taken along the gauge length (the accuracy of the dimension measurements is better than 1%). Although DSGB-10 wt% specimens used a slightly longer gauge length (51 mm vs. 45 mm) due to preparation requirements, all other testing parameters were kept identical. Because elastic modulus is derived from strain normalized to gauge length, this difference introduces no systematic bias into the results. For each composition, three distinct specimens were tested. The parameters recorded included the ultimate tensile strength (in MPa), and the Young's modulus (in GPa).

2.8. Scanning Electron Microscopy (SEM)

The morphological characteristics of the DSG and DSGB composites were examined via Scanning Electron Microscopy (SEM) using a JEOL JSM-5600 scanning electron microscope (JEOL Ltd., Tokyo, Japan), operated with the JEOL SEM Control Software (JEOL Ltd., Tokyo, Japan) and integrated with an Oxford Instruments energy-dispersive X-ray spectrometer (EDS) (Oxford Instruments NanoAnalysis, Abingdon, Oxfordshire, UK). To enhance conductivity and facilitate high-resolution imaging, the specimens were gold-sputtered prior to analysis. Detailed individual and average specimen dimensions and tensile test parameters are summarized in Tables S1 and S2.

3. Results and Discussion

3.1. Cyanoacrylate–Cellulose Interaction Mechanism

The mechanical performance of the fabricated composites is fundamentally rooted in the chemical interaction between the cyanoacrylate adhesive and the cellulosic denim substrate. Cyanoacrylate is an acrylic monomer that undergoes rapid anionic polymerization upon exposure to nucleophilic species, most commonly water molecules or mild bases [24,25]. Denim fabric, being predominantly composed of cotton (~90–95%), is inherently rich in cellulose—a biopolymer characterized by an abundance of hydroxyl groups (–OH) along its molecular backbone (Figure 1a) [32,33]. Upon contact between the cyanoacrylate and the cotton fiber surface, the surface moisture and, potentially, the hydroxyl groups (–OH) of the cellulosic fibers may act as nucleophilic species contributing to the initiation of anionic polymerization of the cyanoacrylate monomer (Figure 1b) [34], though the direct role of cellulosic –OH groups has not been confirmed spectroscopically in the present study, which propagates along the fiber network (Figure 1). The resulting cross-linked poly(cyanoacrylate) matrix forms a continuous, densely bonded phase firmly interlocked with the cellulosic fiber architecture, effectively transforming the flexible textile into a rigid, fiber-reinforced structural composite (Figure 1c) [35]. This in-situ polymerization mechanism, likely facilitated by the chemical functionality of the denim substrate, particularly its surface moisture and cellulosic hydroxyl groups, eliminates the need for external curing agents or elevated processing temperatures, representing a key advantage of this system over conventional epoxy- or polyurethane-based textile composites.

This physical encapsulation and moisture-triggered curing mechanism are macroscopically evidenced by the immediate polymerization of the matrix upon fabric contact and are further supported by the XRD (Section 3.3) and SEM (Section 3.4) analyses.

3.2. Wettability Properties & Contact Angle

Figure 2 depicts the static water contact angle measurements for the fabricated denim–superglue composites, with and without boron carbide (B_4C) reinforcement, together with neat, cured cyanoacrylate as a reference material (Figure 2a). The neat cured cyanoacrylate exhibited a contact angle of 74 ± 4°, whereas the unreinforced denim–superglue composite (DSG, Figure 2b) exhibited a contact angle of 105 ± 4°, representing a significant departure

from the naturally hydrophilic character of untreated denim, which exhibits contact angles approaching 0° due to immediate capillary wicking action. This intrinsic hydrophobicity of the DSG substrate confirms that the cyanoacrylate adhesive fundamentally alters the surface energy of the textile. By sealing the porous fiber network and forming a dense cross-linked polymer layer over the cellulosic substrate, it effectively suppresses the wicking mechanism and forces water to maintain a compact droplet formation on the surface [36].

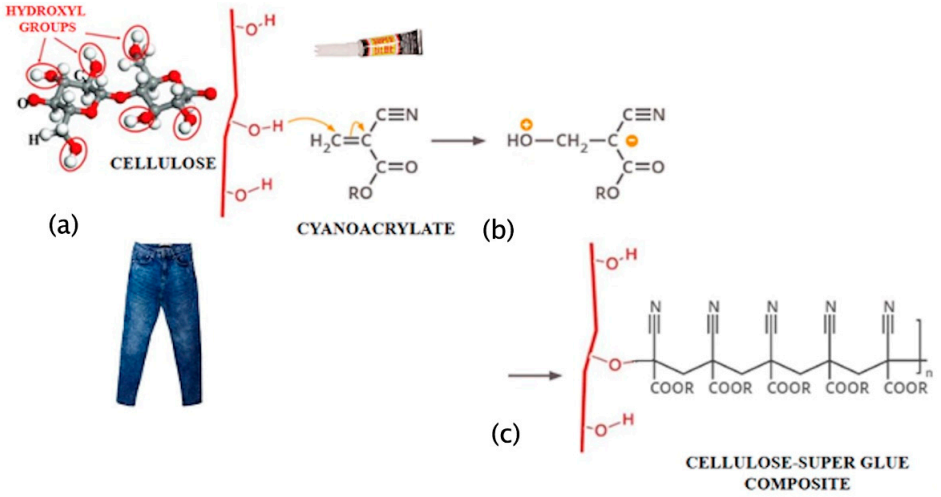


Figure 1. Proposed in situ anionic polymerization mechanism of cyanoacrylate on denim fibers: (**a**) molecular structure of cellulose showing available hydroxyl (–OH) groups (highlighted with red circles; white spheres represent H, red spheres represent O, and grey spheres represent C atoms); (**b**) initiation step through nucleophilic attack of cellulose hydroxyl groups (or surface-bound moisture) on cyanoacrylate monomers (yellow arrow indicates electron pair transfer); and (**c**) propagation step resulting in the formation of a rigid cellulose–poly(cyanoacrylate) composite structure.

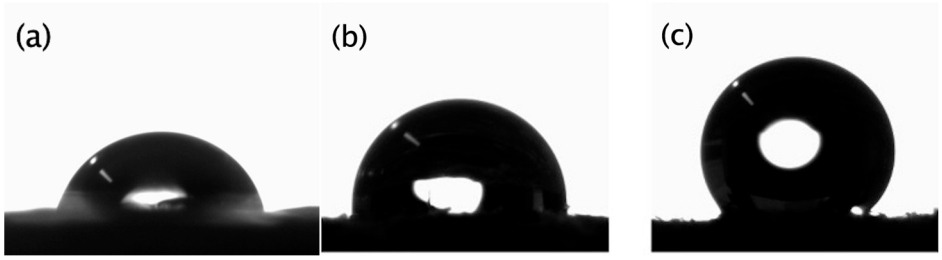


Figure 2. Static water contact angle measurements of (**a**) neat cured cyanoacrylate ($\theta = 74 \pm 4°$), (**b**) the unreinforced denim–cyanoacrylate composite (DSG, $\theta = 105 \pm 4°$), and (**c**) the B_4C-reinforced denim–cyanoacrylate composite (DSGB-7, $\theta = 133 \pm 4°$).

The integration of B_4C particles into the denim–superglue matrix resulted in a marked further enhancement of the water contact angle to $133 \pm 4°$ (Figure 2c), placing the DSGB-7 wt% composite firmly within the strongly hydrophobic regime and approaching the superhydrophobic threshold ($\geq 150°$). This substantial increase of ~28° relative to the unreinforced DSG substrate is attributed to the synergistic interaction between two concurrent mechanisms. First, the B_4C particles introduce a well-defined micro-topography on the composite surface, promoting a Cassie–Baxter wetting regime in which trapped air pockets beneath the droplet reduce the effective solid–liquid contact area, thereby amplifying the apparent contact angle [37]. Second, the progressive coverage of residual polar hydroxyl groups (–OH) on the denim fibers by the ceramic particles further reduces the surface's affinity for water molecules. Recent studies on B_4C composites highlight that their surface performance is highly dependent on preparation processes that govern interfacial bond-

ing and reinforcement distribution [38], consistent with the particle dispersion behavior observed in the SEM analysis of the present study.

Beyond its wetting properties, the incorporation of B_4C significantly enhances the mechanical durability of the composite surface. The exceptional hardness of B_4C particles (~9.5 on the Mohs scale) is expected to contribute to the mechanical robustness of the composite surface within the cyanoacrylate matrix [39], though formal abrasion and durability testing were not performed in the present study. The cyanoacrylate acts as a high-strength structural binder, suggesting that the ceramic particles may remain anchored to the textile fibers under mechanical stress, potentially preserving the micro-topography responsible for the observed hydrophobic behavior, pending validation through dedicated durability testing. Furthermore, the well-known chemical inertness of B_4C ensures that the composite's water-repellent properties are not compromised by environmental exposure or chemical degradation [40]. Consequently, the DSGB composite does not merely offer passive moisture management, but functions simultaneously as a mechanically robust, chemically stable, and moisture-resistant material system. These properties may be of interest for technical textile applications, though their direct relevance to personal protective equipment would require dedicated abrasion, durability, and standardized performance testing beyond the scope of this study.

3.3. X-Ray Diffraction Analysis

The crystalline structure and phase composition of the pristine materials and the fabricated composites (DSG and DSGB) were investigated by X-ray diffraction (XRD), as shown in Figure 3. In particular, the XRD pattern of the pristine denim (D) exhibits the characteristic diffraction peaks of cellulose I, with prominent reflections at $2\theta \approx 14.8^\circ$, 16.5°, and a sharp primary peak at 22.7°, corresponding to the (200) crystallographic plane, thereby confirming the semicrystalline nature of the cotton fibers. According to the literature, denim fabric, being a cotton-based textile, is primarily composed of cellulose (~90–95%), with the remaining fraction consisting of hemicellulose, lignin, and natural waxes [32,39]. These components dictate its semi-crystalline behavior, as the crystalline regions of cellulose are embedded within an amorphous matrix of hemicellulose and lignin. Recent studies on the valorization of textile waste emphasize that the structural integrity of these natural fibers is critical for the mechanical performance of reinforced composites [41].

On the other hand, the reference Boron Carbide (B_4C) powder used as the ceramic additive in the composite exhibits a highly crystalline profile with sharp Bragg reflections at $2\theta \approx 23.5^\circ$, 35° and 38°, consistent with its rhombohedral structure as reported in ceramic filler research [42]. As observed in Figure 3, the presence of boron carbide becomes clearly detectable in the DSGB samples containing 7 wt% and 10 wt% B_4C, as evidenced by Bragg reflections at $2\theta \approx 23.5^\circ$ (manifested as an asymmetry of the main peak at higher angles) as well as at 35° and 38°, which appear as clearly resolved new diffraction peaks. In addition, a clear concentration dependence is observed, as the relative intensity of the characteristic B_4C peaks increases proportionally with the filler loading. On the other hand, following the incorporation of the cyanoacrylate matrix into the denim structure, the DSG and DSGB composites maintain the characteristic cellulose diffraction peaks, although slight peak broadening and an increase in the amorphous background are observed. This is attributed to the intrinsically amorphous nature of the superglue polymer, which partially encapsulates the denim fibers and exhibits a broad scattering contribution mainly centered around $2\theta \approx 15^\circ$ and 32°, as also evidenced by the diffraction pattern (Figure 3) of the neat superglue phase (SG). The simultaneous presence of both cellulose and B_4C diffraction peaks, together with the absence of significant peak shifts, suggests that the incorporation of the cyanoacrylate matrix and ceramic filler into the denim structure primarily results in physi-

cal integration and interfacial interactions, without the formation of new crystalline phases or significant structural transformations. This interpretation is further supported by the observed peak broadening and increased amorphous background, which are attributed to partial encapsulation of the cellulose fibers by the amorphous polymer phase, in agreement with recent findings on high-strength textile-reinforced polymer composites [43].

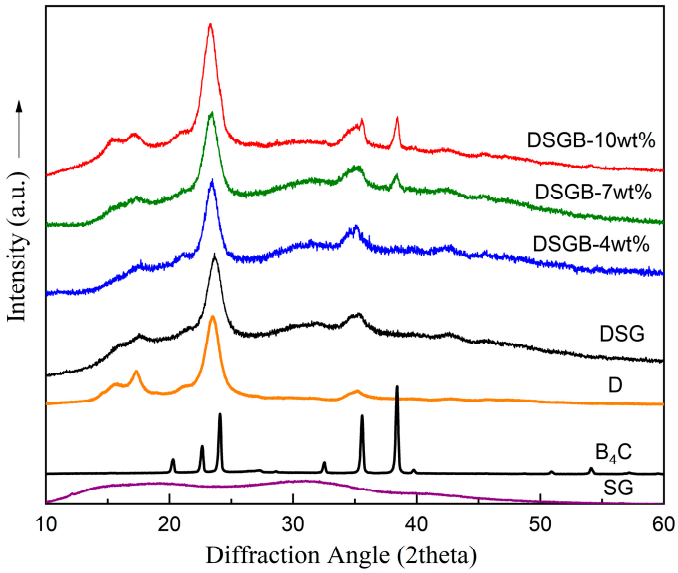


Figure 3. XRD patterns of pure boron carbide (B_4C), raw denim fabric (D), superglue (SG), superglue–denim composite (DSG), and superglue–denim composite with varying B_4C concentrations (4 wt%, 7 wt%, and 10 wt%) (DSGB).

3.4. Scanning Electron Microscopy (SEM) Analysis

The surface morphology of the raw denim and the fabricated composites was examined via scanning electron microscopy (SEM), as presented in Figure 4. The pristine denim fabric (D) consists of distinct, relatively smooth, and well-defined cotton fibers with a characteristic twisted structure. Upon application of the cyanoacrylate adhesive (DSG), the fiber surfaces become coated with a continuous adhesive layer, resulting in partial fiber encapsulation and the formation of a more integrated fiber–polymer network. On the other hand, when 7 wt% B_4C particles are deposited onto the pristine denim fabric, the SEM micrographs (Figure 4c) reveal a relatively homogeneous distribution of fine ceramic particles over the cotton fiber surfaces. The particles appear well dispersed and predominantly isolated, suggesting that this loading level does not promote significant agglomeration. Following cyanoacrylate impregnation (Figure 4d), the B_4C particles become firmly embedded within the polymer phase, which forms continuous bridges between adjacent fibers, effectively anchoring the ceramic particles while preserving their relatively uniform distribution throughout the fibrous network. This configuration promotes efficient particle–matrix–fiber interfacial contact, which is consistent with the enhanced mechanical performance observed for the DSGB-7 wt% composition.

At the higher B_4C loading of 10 wt%, however, the microstructure changes markedly (Figure 4e). Large particle-rich regions and extensive agglomerates become clearly evident, indicating that the ceramic particle content exceeds the dispersion capability of the available cyanoacrylate phase, resulting in an increasingly heterogeneous filler distribution. Higher-magnification micrographs (Figure 4f), reveal the formation of compact B_4C clusters in which many particles are in direct particle-to-particle contact rather than being individually dispersed within the polymer matrix. These agglomerates may act as stress concentration sites, disrupting load transfer efficiency, and likely represent a major contributing factor to

the deterioration in tensile strength and stiffness observed for the DSGB-10 wt% composite. Other unmeasured factors, such as local variations in matrix impregnation, porosity, fiber distribution, and specimen thickness, cannot be excluded as additional contributors to this decline.

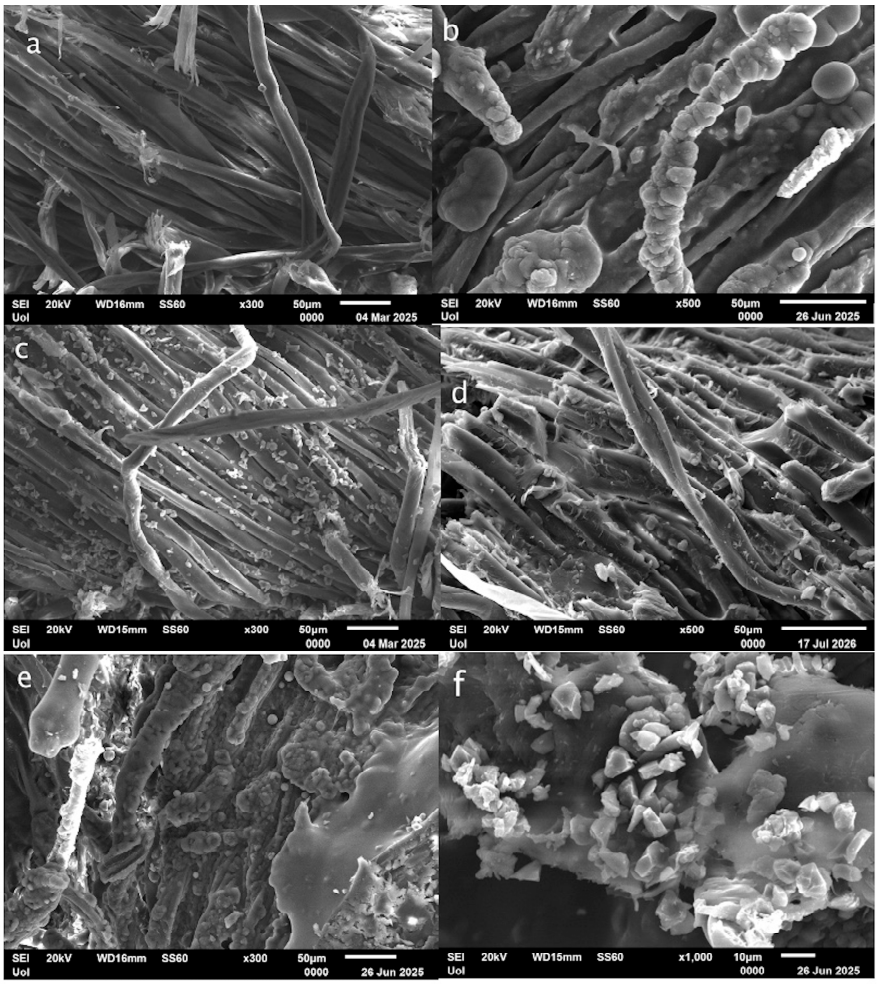


Figure 4. SEM micrographs of: (**a**) pristine denim fabric (D), (**b**) denim fabric impregnated with cyanoacrylate (DSG), (**c**) pristine denim fabric with deposited B_4C particles (7 wt%), (**d**) denim–cyanoacrylate composite containing 7 wt% B_4C (DSGB-7), (**e**) denim–cyanoacrylate composite containing 10 wt% B_4C (DSGB-10), and (**f**) higher-magnification image of (**e**), highlighting the distribution and agglomeration of B_4C particles.

These morphological observations are in good agreement with the structural data obtained from the XRD analysis. The clear, individualized fibers observed in the SEM of the D correspond to the sharp, well-defined peaks of Cellulose I in the XRD pattern. The encapsulation of fibers by the superglue, observed in the SEM, correlates with the increased amorphous background and slight peak broadening in the DSG and DSGB XRD patterns, confirming the presence of the non-crystalline polymer matrix. Furthermore, the progressive increase in B_4C particle density and the appearance of particle clusters in the SEM micrographs is consistent with the proportional increase in the intensity of the B_4C Bragg reflections in the XRD patterns. This correlation between surface morphology and crystalline structure confirms that the boron carbide filler was successfully incorporated into the superglue–denim system, retaining its crystalline identity while physically reinforcing the composite structure, with the 7 wt% formulation representing the optimum threshold where crystalline integration is maximized without compromising particle dispersion. The transition from a well-dispersed microstructure at 7 wt% to the heavily

particle-populated surface observed at 10 wt% indicates that the composite has reached its practical particle-loading limit. The limited amount of cyanoacrylate matrix is no longer sufficient to uniformly disperse and bind the increased amount of B_4C, leading to extensive particle accumulation and agglomeration. It is acknowledged that direct measurements of bulk density, open porosity, and areal weight, as well as cross-sectional SEM analysis of the through-thickness matrix and filler distribution, were not performed in the present study. These characterizations represent important priorities for future investigation to provide a more complete microstructural and physical description of the composite system.

3.5. Dynamic Impact Response

The dynamic impact response of the fabricated composites was evaluated by measuring the peak contact force (kN) generated during drop-weight impact events, as illustrated in Figures 5 and 6. The applied experimental configuration employed an instrumented impactor equipped with a load cell, which records the force developed at the impactor–specimen interface. Therefore, the measured peak contact force represents the local impact interaction between the impactor and the composite specimen and should not be interpreted as transmitted force through the specimen to a supporting structure. The analysis presented herein focuses on the comparative effect of B_4C incorporation on the impact response of the investigated composites under the specific laboratory conditions employed. Prior to discussing the mechanical response of the fabricated composites, it is instructive to consider the intrinsic mechanical characteristics of the constituent materials. Denim fabric, as a woven cotton textile, exhibits a characteristically flexible and anisotropic mechanical behavior, with tensile strength values typically ranging from 10 to 50 MPa depending on weave architecture, fiber orientation, and yarn count [44]. Although denim possesses reasonable load-bearing capacity along the warp direction, it offers virtually no resistance to out-of-plane deformation or localized penetration in the absence of a rigid reinforcing phase. Conversely, cured cyanoacrylate adhesive forms a highly cross-linked glassy polymer network that exhibits high stiffness but limited ductility, which may restrict energy dissipation under dynamic loading conditions [45].

Consequently, neither constituent alone provides the combination of mechanical characteristics required for the targeted composite response: denim offers flexibility and fibrous reinforcement but limited out-of-plane rigidity, whereas neat cyanoacrylate provides high stiffness but limited ductility under dynamic loading conditions. The denim–cyanoacrylate composite system was therefore designed to combine the complementary characteristics of both constituents, where the fibrous denim network contributes structural reinforcement and damage tolerance, while the cyanoacrylate matrix enhances rigidity and load transfer efficiency. This response is further modified by the incorporation of B_4C ceramic particles, as indicated by the mechanical and dynamic impact results presented in Figures 6 and 7.

The experimental results shown in Figure 6b reveal a distinct transition in the material's impact response as boron carbide (B_4C) content increases. The unreinforced sample DSG (0 wt% B_4C) recorded the lowest peak contact force of 0.34 kN, corresponding to a more compliant response under the applied impact conditions, where the denim–superglue matrix, still relatively compliant in the absence of ceramic filler, can accommodate impact loading through localized deformation of the fiber network and polymer matrix. The contact force increased progressively and monotonically with B_4C content, reaching 0.69 kN (4 wt%), 0.92 kN (7 wt%), and 1.31 kN (10 wt%), reflecting a progressive stiffening and increasingly direct load transfer through the composite thickness, rather than being interpreted as direct evidence of improved energy attenuation.

It is important to note that the cyanoacrylate (superglue) does not merely coat the denim fibers but undergoes in-situ anionic polymerization initiated by surface moisture

and the hydroxyl groups of the cellulosic fibers, yielding a rigid, densely cross-linked polymeric network firmly interlocked with the denim fiber architecture and transforming the composite from a flexible textile into a semi-rigid to rigid structural panel. Consequently, as B_4C loading increases, the composite exhibits an increasingly stiff impact response rather than behaving as a flexible cushioning material, in which the incorporation of ceramic particles further restricts the residual elasticity of the cross-linked polymer–fiber network and promotes more direct load transfer through the panel thickness.

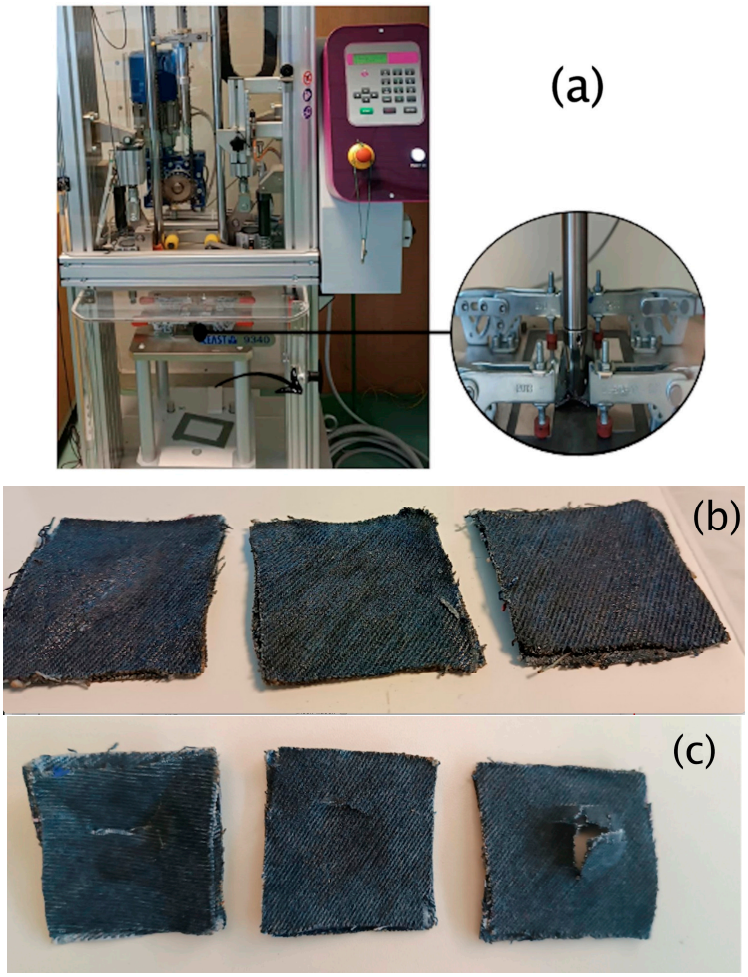


Figure 5. Drop-weight impact testing of the denim–superglue composites: (**a**) experimental setup using the Instron CEAST 9340 Drop Tower with a detailed inset showing the clamping fixture and hemispherical impactor position (**upper**); (**b**) representative DSGB-7 wt% specimens prior to impact testing (**middle**); and (**c**) post-impact DSGB-7 wt% specimens showing progressive damage modes across three independent replicates, ranging from surface indentation and localized fiber deformation to full perforation, following 10 J drop-weight impact loading (**bottom**).

Figure 6a shows representative load–displacement curves from drop-weight impact tests at 10 J impact energy for denim–superglue composites with varying B_4C concentrations (0, 4, 7, and 10 wt%; curves vertically offset for clarity). All specimens show an initial elastic loading segment followed by oscillations superimposed on a broader force envelope, progressive damage evolution during impact, including possible fiber fracture, delamination, and interfacial debonding, rather than a single catastrophic failure. A clear trend emerges with increasing B_4C content: peak contact force (force–displacement work) and the area under the curve (absorbed energy) increase progressively from DSG to DSGB (10 wt%). The unreinforced DSG sample shows the lowest, most irregular response with pronounced sawtooth-like oscillations, indicating a more compliant response with intermittent damage

events. The B_4C-reinforced composites, especially at 7 and 10 wt%, show a smoother, higher-amplitude envelope, indicating a stiffer impact response and more efficient load transfer within the composite structure. This behavior reflects the reinforcing role of the rigid B_4C particles: by increasing local matrix stiffness and hardness, they modify the deformation response of the composite and may contribute to a more distributed damage evolution, rather than highly localized deformation as observed in DSG. However, the specific microstructural damage mechanisms cannot be fully established from the present impact measurements alone. This increase in peak contact force reflects the increased stiffness and more direct load transfer within the composite, rather than direct evidence of improved impact attenuation.

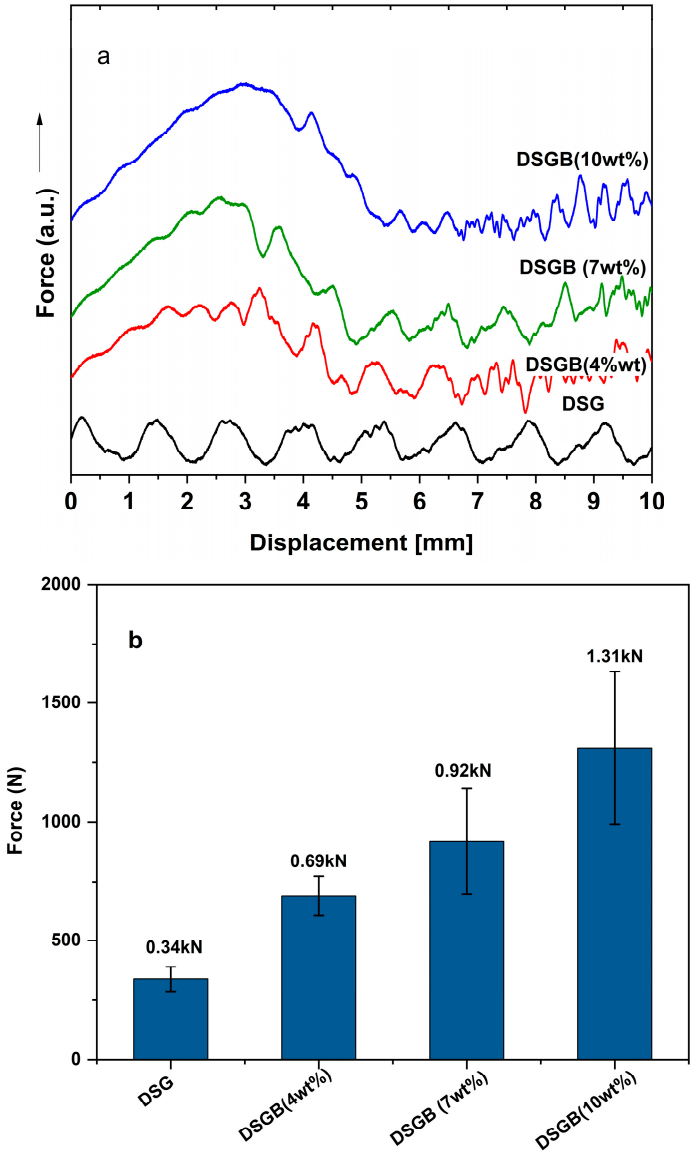


Figure 6. (**a**) Representative load–displacement curves of denim–superglue composites with various boron carbide (B_4C) concentrations (0, 4, 7, and 10 wt%) under drop-weight impact loading at 10 J impact energy, showing progressive layer-by-layer damage and increasing load-bearing capacity with B_4C content. (**b**) Peak contact force of the same composites, calculated as the mean value of three independent specimens per composition, with error bars representing the standard deviation (SD). The measured peak contact force values are presented for comparative evaluation of the effect of B_4C incorporation on the impact response of the investigated composites under the applied experimental conditions.

The energy absorbed by each specimen during the impact test was calculated as the area under the Force–Displacement curve. This value represents the mechanical work associated with the recorded impact response under the present experimental configuration. The DSG specimen exhibited a lower calculated mechanical work value, consistent with its more compliant response and limited resistance under the applied impact conditions. In contrast, the incorporation of boron particles into the DSGB formulation resulted in a marked increase in calculated force–displacement work, which scaled with additive content: 3.0 ± 0.3 J for DSGB (4 wt%), 4.1 ± 0.5 J for DSGB (7 wt%), and 5.8 ± 0.6 J for DSGB (10 wt%). This trend is consistent with the increase in peak force and indicates that higher B_4C loading modifies the impact response by increasing stiffness and load transfer capability; however, it should not be interpreted as direct evidence of improved protective performance or impact attenuation without standardized transmitted-force measurements.

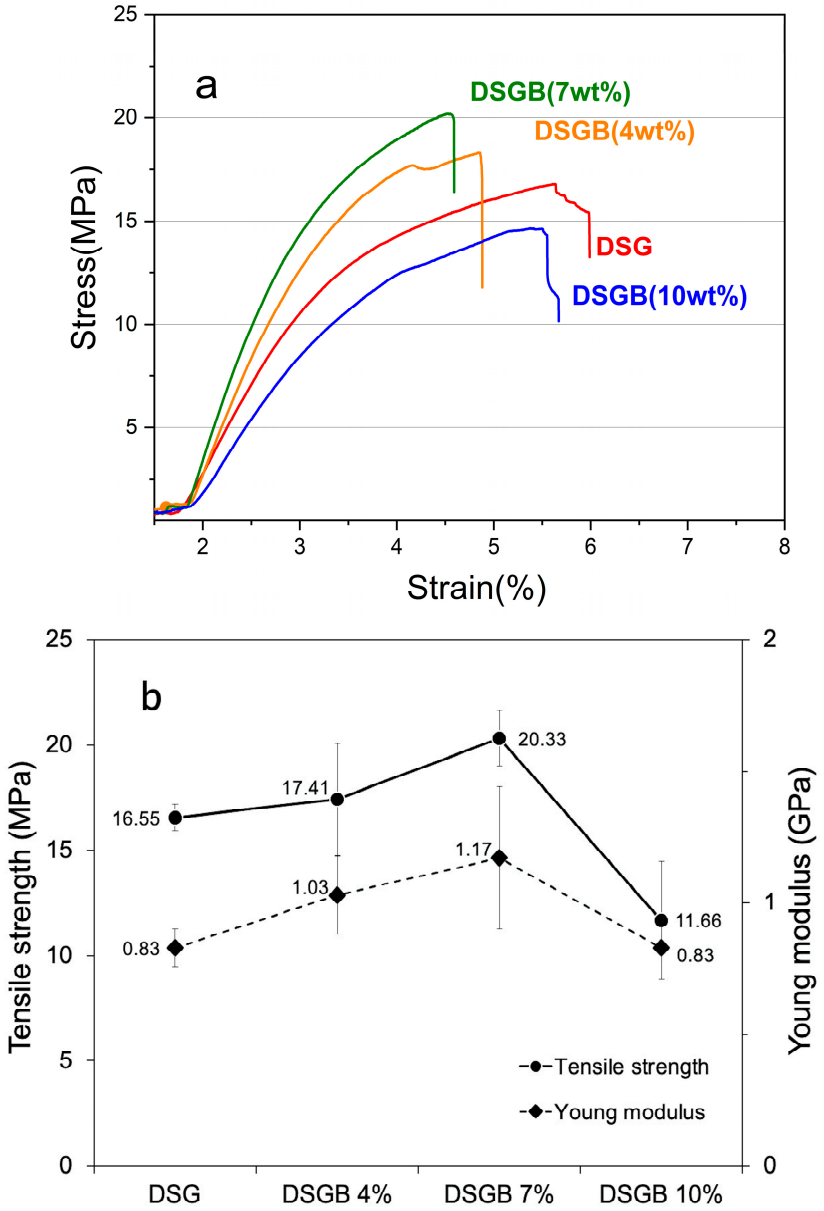


Figure 7. Tensile properties of the denim–superglue composites: (**a**) representative stress–strain curves of B_4C-reinforced composites (4, 7, and 10 wt%), (**b**) average values of tensile strength and Young's modulus with standard deviation (SD) obtained from three independent tensile measurements (n = 3).

Given this rigid, ceramic-reinforced character, the composite was further evaluated in terms of its dynamic impact response under the present laboratory conditions. The measured peak contact force values were not directly compared with impact-protection standards, such as EN 1621-1 [46], EN 1621-2 [47], and ANSI/ISEA 138 [48], because these standards employ different test configurations in which transmitted force is measured through a backing support using specific specimen geometries and transducer locations. Although these standards provide relevant context for protective equipment testing, direct numerical comparison with the present contact-force measurements is not technically justified. It is critical to note that present experiments quantify the force developed at the impactor–specimen interface rather than the force transmitted through the specimen to a protected body or support structure.

This behavior may be attributed to a synergistic interaction between the cross-linked denim–cyanoacrylate matrix and the B_4C ceramic reinforcement. The rigid, fiber-reinforced polymer network promotes stress redistribution across the composite surface and enhances resistance to localized deformation. Although the increasing absorbed energy with B_4C content is consistent with an enhanced impact response, the present study does not directly establish the specific microstructural energy-dissipation mechanisms, as porosity, B_4C volume fraction, and through-thickness particle distribution were not measured. Moreover, the increase in peak contact force should be interpreted primarily as evidence of increased composite stiffness and more efficient load transfer, whereas calculated force–displacement work represents the mechanical work associated with the recorded impact event. These quantities describe different aspects of the impact response and should not be interpreted as direct evidence of the same mechanism. These findings, together with the SEM and XRD observations, suggest that the B_4C composites merit further investigation as candidate materials for protective textile applications. However, this interpretation is based on small-scale, non-standardized specimens, and any conclusions regarding practical protective performance remain preliminary pending validation through appropriate standardized testing procedures.

3.6. Effect of B_4C Loading on Tensile Performance

The tensile behavior of the DSG and DSGB composites was systematically investigated to evaluate the reinforcing effect of boron carbide (B_4C) loading. The representative stress–strain curves and the corresponding Young's modulus values are presented in Figure 7 (with individual and average tensile data provided in Tables S1 and S2, respectively).

As illustrated in Figure 7a, the incorporation of B_4C up to 7 wt% progressively enhances the ultimate tensile strength of the composites. The unreinforced denim–cyanoacrylate composite (DSG) exhibited a peak stress of approximately 16.55 ± 0.63 MPa, increasing to 17.41 ± 2.68 MPa at 4 wt%, and reaching its maximum value of 20.33 ± 1.33 MPa at 7 wt% B_4C, representing a notable improvement in the load-bearing capacity of the textile-reinforced system. This strengthening is primarily attributed to the efficient load transfer from the cyanoacrylate–denim matrix to the high-strength ceramic particles [49,50]. The Young's modulus (Figure 7b) followed a similar trend, increasing from 0.83 GPa (0 wt%) to 1.03 GPa (4 wt%) and reaching a maximum of 1.17 GPa at 7 wt%, confirming that the B_4C particles effectively reinforce the polymer-fiber network up to this loading and significantly increase the material's rigidity [36]. For reference, the raw, unimpregnated denim fabric (D) exhibited a highly non-linear stress–strain response characteristic of woven textile structures, with substantially lower strength and stiffness compared with the cyanoacrylate-impregnated composites. This behavior highlights the significant contribution of the cyanoacrylate matrix in improving load transfer efficiency and enhancing the overall mechanical performance of the composite system. The high particle density

observed in the SEM micrographs supports this, as the ceramic filler creates a robust mechanical interlocking mechanism with the denim fibers. Interestingly, both the tensile strength and the stiffness exhibited a marked decline at the 10 wt% B_4C loading. The Young's modulus decreased to 0.83 GPa, indicating the loss of the stiffening effect provided at 7 wt% B_4C and matching the value of the unreinforced denim–cyanoacrylate composite. In parallel, the ultimate tensile strength and strain at break were substantially reduced compared to the 7 wt% sample. This simultaneous deterioration in both strength and stiffness is consistent with a well-documented threshold phenomenon in composite science, commonly associated with filler agglomeration [49–51], as supported by the SEM observations of particle clustering at this loading level (Section 3.4). Such agglomerates may act as stress concentrators and microstructural heterogeneities, disrupting load transfer efficiency and potentially promoting micro-crack initiation. However, agglomeration cannot be considered the only contributing factor, as variations in matrix impregnation quality, porosity, fiber distribution, and specimen thickness were not independently quantified in this study and may also have contributed to the observed decline in mechanical performance. The lower Young's modulus of DSGB-10 wt% is mainly due to B_4C agglomeration and resulting stress concentrations (Section 3.4). Although it has been tested with a slightly longer gauge length (51 mm vs. 45 mm) without introducing systematic bias, future studies should maintain a uniform gauge length to avoid any methodological ambiguity. Furthermore, at this concentration, the matrix may become insufficient to fully wet and encapsulate the high surface area of the particles and fibers, leading to weakened interfacial bonding and a less cohesive, more defect-prone network overall [49].

A critical finding of this study is the contrast between the static (tensile) and dynamic (impact) mechanical responses. Although the 10 wt% sample underperformed in terms of both tensile strength and stiffness due to agglomeration-induced defects, it exhibited the highest peak contact force (1.31 kN), reflecting maximum stiffness and direct load transfer rather than optimal energy attenuation. This suggests that under high-velocity impact, the sheer volumetric density of the B_4C filler—rather than its uniform dispersion or interfacial bonding quality—governs the energy-dissipation response, overshadowing the structural weaknesses that dominate under slow-rate tensile loading [52]. In other words, the stiffening response under impact is primarily governed by particle hardness and packing density, whereas tensile performance is critically dependent on dispersion quality and fiber–matrix adhesion—explaining why the two mechanical responses diverge so markedly at high filler content.

To evaluate the mechanical and impact-response performance of the present composites, a comparison with relevant literature analogs and protective-material benchmarks is warranted. Recycled denim-reinforced polypropylene composites reported by Webo et al. achieved tensile strengths of up to 57 MPa at high fiber fractions (84 wt%), although their fabrication required hot-press processing and virgin thermoplastic matrices [19]. Denim/PLA composites fabricated by hand layup exhibited tensile strengths of up to 75.76 MPa and tensile moduli of 4.65 GPa using multiple fabric layers [53], while denim/jute hybrid thermoplastic composites reported tensile moduli of approximately 2.1 GPa [54]. In comparison, the present denim–superglue–B_4C (DSG) composites achieved tensile strengths of up to 20.33 $\pm$ 1.33 MPa and moduli of up to 1.17 GPa at relatively low B_4C loadings. These lower mechanical properties compared with highly reinforced or multilayer systems are expected, considering the single-impregnation, room-temperature curing, proof-of-concept fabrication approach adopted in this study. A potential limitation of this screening study is the relatively small sample size (n = 3), which is sufficient to identify material trends but should be considered when interpreting the absolute property values.

The main advantage of the present DSGB composites lies not in achieving the highest tensile performance, but in combining a simple, low-energy fabrication route, a fully waste-derived denim substrate, and the incorporation of B_4C reinforcement to provide enhanced functional attributes, including hydrophobicity and impact-response characteristics. The impact experiments performed in this study were conducted on small laboratory specimens using an instrumented impactor that measured the contact force at the impactor–specimen interface. Consequently, the measured force should not be directly compared with the transmitted-force values specified in standardized protective equipment test methods, which employ different specimen geometries, support conditions, transducer locations, and testing protocols. The present impact results should therefore be interpreted as comparative laboratory-scale measurements demonstrating the relative influence of B_4C loading on the impact response of the composites, providing a basis for further material optimization and subsequent evaluation under standardized testing conditions.

4. Conclusions

The present study successfully demonstrated the development of a high-performance, sustainable composite material through the upcycling of waste denim fabric into a cyanoacrylate matrix reinforced with boron carbide (B_4C) microparticles. Structural and morphological analyses using XRD and SEM confirmed the effective encapsulation of the fibrous network and the successful incorporation of the ceramic filler. However, a transition toward localized particle agglomeration was observed at the 10 wt% loading level. Mechanical evaluation revealed a distinct, non-monotonic relationship between filler concentration and mechanical performance. A B_4C loading of 7 wt% was identified as the optimum composition for static mechanical performance, achieving a tensile strength of approximately 20.33 ± 1.33 MPa and a Young's modulus of 1.17 GPa. Further increase in filler content resulted in a deterioration of both properties, with the Young's modulus decreasing to 0.83 GPa, a value comparable to that of the unreinforced composite (0.83 GPa). This decline likely reflects agglomeration-induced stress concentrations as a major contributing factor, alongside other unquantified parameters such as impregnation quality, porosity, and fiber distribution. Conversely, under dynamic impact loading, the material exhibited a progressive transition from a more compliant response to a stiffer impact response, with the peak contact force increasing monotonically from 0.34 kN (0 wt%) to 1.31 kN (10 wt%). This increase in peak contact force is consistent with the increasing stiffness of the composite resulting from B_4C incorporation and reflects changes in the impact response under the present experimental configuration. Because the force was measured at the impactor–specimen interface, these values represent contact force and should not be directly compared with transmitted-force limits defined by standardized personal protective equipment test methods. Furthermore, surface wettability characterization revealed a significant enhancement in hydrophobicity following B_4C incorporation, with the static water contact angle increasing from $105 \pm 4^\circ$ (DSG) to $133 \pm 4^\circ$ (DSGB), consistent with a Cassie–Baxter wetting regime promoted by the ceramic-induced surface microtopography.

Overall, this study presents a proof-of-concept strategy for upcycling textile waste into value-added engineering materials, demonstrating preliminary improvements in mechanical, wettability, and impact-response characteristics. These findings indicate potential for future protective textile applications; however, confirmation of practical relevance to personal protective equipment requires standardized, full-scale testing and validation beyond the scope of the present study.

Supplementary Materials: The following supporting information can be downloaded at: https://www.mdpi.com/article/10.3390/eng7080396/s1. Table S1: Individual geometric characteristics and tensile properties of the tested denim–cyanoacrylate composite specimens with different B_4C contents (0, 4, 7, and 10 wt%). Table S2: Mean geometric characteristics and tensile properties of the tested denim–cyanoacrylate composite specimens with different B_4C contents (0, 4, 7, and 10 wt% B_4C).

Author Contributions: Conceptualization, M.A.K., A.B.B. and C.G.; methodology, M.A.K.; formal analysis, M.A.K., C.G. and S.A.; investigation, M.A.K., C.G., S.A., D.M. and A.A.; resources, M.A.K., C.E.S. and A.A.; data curation, M.A.K., C.G., S.A. and D.M.; writing—original draft preparation, C.G.; writing—review and editing, M.A.K., C.E.S. and A.B.B.; supervision, M.A.K.; project administration, M.A.K. and C.G.; funding acquisition, M.A.K. All authors have read and agreed to the published version of the manuscript.

Funding: This work was carried out within the framework of the Action 'Flagship Research Projects in challenging interdisciplinary sectors with practical applications in Greek industry', implemented through the National Recovery and Resilience Plan Greece 2.0 and funded by the European Union—NextGenerationEU (project code: TAEDR-0535821).

Institutional Review Board Statement: Not applicable.

Informed Consent Statement: Not applicable.

Data Availability Statement: The original contributions presented in this study are included in the article/Supplementary Materials. Further inquiries can be directed to the corresponding authors.

Acknowledgments: The authors gratefully acknowledge A. Paipetis for providing access to the laboratory facilities where the Impact Attenuation Performance measurements were carried out. During the preparation of this manuscript/study, the authors used ChatGPT (the free version) for the purposes of English language improvement. The authors have reviewed and edited the output and take full responsibility for the content of this publication.

Conflicts of Interest: The authors declare no conflicts of interest.

Abbreviations

ANSI	American National Standards Institute
ASTM	American Society for Testing and Materials
B_4C	Boron Carbide
CEN	European Committee for Standardization
COD	Crystallography Open Database
DSG	Denim–Superglue
DSGB	Denim–Superglue–Boron Carbide
EDS	Energy-Dispersive X-ray Spectroscopy
ISEA	International Safety Equipment Association
PPE	Personal Protective Equipment
SEM	Scanning Electron Microscopy
wt%	Weight Percent
XRD	X-ray Diffraction

References

1. Grand View Research. Denim Jeans Market Size & Trends. Available online: https://www.grandviewresearch.com/industry-analysis/denim-jeans-market (accessed on 26 May 2025).
2. Statista. Market Size of Denim Jeans Worldwide from 2021 to 2026. Available online: https://www.statista.com/statistics/1368005/global-units-of-denim-jeans-market (accessed on 26 May 2025).
3. Akı, S.U.; Candan, C.; Nergis, B.; Önder, N.S. Understanding Denim Recycling: A Quantitative Study with Lifecycle Assessment Methodology. In *Waste in Textile and Leather Sectors*; Körlü, A., Ed.; IntechOpen: London, UK, 2020. [CrossRef]

4. Tharmarajah, N.; Shahbaz, K.; Baroutian, S. Textile Waste Pretreatment for Anaerobic Digestion: A Review and Technology Feasibility Study. *J. Chem. Technol. Biotechnol.* **2024**, *99*, 2213–2227. [CrossRef]
5. Periyasamy, A.P.; Periyasami, S. Critical Review on Sustainability in Denim: A Step Toward Sustainable Production and Consumption of Denim. *ACS Omega* **2023**, *8*, 4472–4490. [CrossRef] [PubMed]
6. Li, Z.; Zhang, M.; Li, F.; Shi, S.; Wang, S.; Gao, C.; Li, Y. Recycling of Waste Denim: A Stepwise Utilisation Strategy for Clean Decolourisation, Opening and Degradation. *Waste Manag.* **2025**, *198*, 12–20. [CrossRef] [PubMed]
7. Sanjrani, M.A.; Gang, X.; Mirza, S.N.A. A Review on Textile Solid Waste Management: Disposal and Recycling. *Waste Manag. Res.* **2025**, *43*, 522–539. [PubMed]
8. Luiken, A.; Bouwhuis, G. Recovery and Recycling of Denim Waste. In *Denim Manufacture, Finishing and Applications*; Paul, R., Ed.; Woodhead Publishing: Cambridge, UK, 2015; pp. 527–540.
9. Radhakrishnan, S. Denim Recycling. In *Textiles and Clothing Sustainability*; Muthu, S.S., Ed.; Springer: Singapore, 2017; pp. 79–125.
10. Yousef, S.; Tatariants, M.; Tichonovas, M.; Kliucininkas, L.; Lukošiūtė, S.-I.; Yan, L. Sustainable Green Technology for Recovery of Cotton Fibers and Polyester from Textile Waste. *J. Clean. Prod.* **2020**, *254*, 120078. [CrossRef]
11. Xie, X.; Hong, Y.; Zeng, X.; Dai, X.; Wagner, M. A Systematic Literature Review for the Recycling and Reuse of Wasted Clothing. *Sustainability* **2021**, *13*, 13732. [CrossRef]
12. Juanga-Labayen, J.P.; Labayen, I.V.; Yuan, Q. A Review on Textile Recycling Practices and Challenges. *Textiles* **2022**, *2*, 174–188. [CrossRef]
13. Kanan, M.; Wannassi, B.; Barham, A.S.; Ben Hassen, M.; Assaf, R. The Quality of Blended Cotton and Denim Waste Fibres: The Effect of Blend Ratio and Waste Category. *Fibers* **2022**, *10*, 76. [CrossRef]
14. Haque, M.S.; Sharif, A. Processing and Characterization of Waste Denim Fiber Reinforced Polymer Composites. *Int. J. Innov. Sci. Mod. Eng.* **2014**, *2*, 24–28.
15. Echeverria, C.A.; Handoko, W.; Pahlevani, F.; Sahajwalla, V. Cascading Use of Textile Waste for the Advancement of Fibre Reinforced Composites for Building Applications. *J. Clean. Prod.* **2019**, *208*, 1524–1536. [CrossRef]
16. Meng, X.; Fan, W.; Ma, Y.; Wei, T.; Dou, H.; Yang, X.; Tian, H.; Yu, Y.; Zhang, T.; Gao, L. Recycling of Denim Fabric Wastes into High-Performance Composites Using the Needle-Punching Nonwoven Fabrication Route. *Text. Res. J.* **2020**, *90*, 695–709.
17. Patti, A.; Cicala, G.; Acierno, D. Eco-Sustainability of the Textile Production: Waste Recovery and Current Recycling in the Composites World. *Polymers* **2021**, *13*, 134. [PubMed]
18. Wang, S.; Zhang, T.; Zhang, X.; Ge, S.; Fan, W. Development of 3D Needled Composite from Denim Waste and Polypropylene Fibers for Structural Applications. *Constr. Build. Mater.* **2022**, *314*, 125583. [CrossRef]
19. Webo, W.; Khoathane, M.C.; Mhike, W.; Mohlamonyane, R.S. Enhancing Sustainability: Composite Materials from Recycled HDPE and Denim Fillers. *Polym. Eng. Sci.* **2025**, *65*, 2395–2404. [CrossRef]
20. Khan, R.M.W.U.; Seyam, A.F.M.; Hussain, M.; Nawab, Y. Valorizing Denim and Polyethylene Sheet Waste to Fiber-Reinforced Composites. *Polym. Compos.* **2025**, *46*, 12091–12111. [CrossRef]
21. Zonatti, W.F.; Guimarães, B.M.G.; Duleba, W.; Ramos, J.B. Thermoset Composites Reinforced with Recycled Cotton Textile Residues. *Text. Cloth. Sustain.* **2015**, *1*, 1. [CrossRef]
22. Tiuc, A.-E.; Vermeşan, H.; Gabor, T.; Vasile, O. Improved Sound Absorption Properties of Polyurethane Foam Mixed with Textile Waste. *Energy Procedia* **2016**, *85*, 559–565. [CrossRef]
23. Raj, M.; Fatima, S.; Tandon, N. Recycled Materials as a Potential Replacement to Synthetic Sound Absorbers: A Study on Denim Shoddy and Waste Jute Fibers. *Appl. Acoust.* **2020**, *159*, 107070. [CrossRef]
24. Raja, P.R. Cyanoacrylate Adhesives: A Critical Review. *Rev. Adhes. Adhes.* **2016**, *4*, 398–416. [CrossRef]
25. Samuel, H.S.; Nweke-Maraizu, U.; Etim, E.E. Cyanoacrylate Chemistry and Polymerization Mechanisms. *Prog. Chem. Biochem. Res.* **2024**, *7*, 129–142.
26. Boldin, M.S.; Berendeev, N.N.; Melekhin, N.V.; Popov, A.A.; Nokhrin, A.V.; Chuvildeev, V.N. Review of Ballistic Performance of Alumina: Comparison of Alumina with Silicon Carbide and Boron Carbide. *Ceram. Int.* **2021**, *47*, 25201–25213. [CrossRef]
27. Silveira, P.H.P.M.D.; Silva, T.T.D.; Ribeiro, M.P.; Rodrigues de Jesus, P.R.; Credmann, P.C.R.D.S.; Gomes, A.V. A Brief Review of Alumina, Silicon Carbide and Boron Carbide Ceramic Materials for Ballistic Applications. *Acad. Lett.* **2021**, 3742.
28. Ka, J.; Kim, K.H.; Choi, W.; Jung, S.; Lee, T.H.; Kim, H.S.; Lee, H.; Lee, J.H. Improving the Fracture Toughness of Boron Carbide via Minor Additions of SiC and TiB_2 Through Hot-Press Sintering. *Materials* **2024**, *17*, 6233. [CrossRef] [PubMed]
29. Avcıoğlu, S.; Buldu, M.; Kaya, F.; Üstündağ, C.B.; Kam, E.; Menceloğlu, Y.Z.; Kaptan, H.Y.; Kaya, C. Processing and Properties Boron Carbide (B_4C) Reinforced LDPE Composites for Radiation Shielding. *Ceram. Int.* **2020**, *46*, 343–352. [CrossRef]
30. *ASTM D7136/D7136M-25*; Standard Test Method for Measuring the Damage Resistance of a Fiber-Reinforced Polymer Matrix Composite to a Drop-Weight Impact Event. ASTM International: West Conshohocken, PA, USA, 2025.
31. *ASTM D3039/D3039M-17(2025)*; Standard Test Method for Tensile Properties of Polymer Matrix Composite Materials. ASTM International: West Conshohocken, PA, USA, 2025.

32. Ruiz-Caldas, M.-X.; Carlsson, J.; Sadiktsis, I.; Jaworski, A.; Nilsson, U.; Mathew, A.P. Cellulose Nanocrystals from Postconsumer Cotton and Blended Fabrics: A Study on Their Properties, Chemical Composition, and Process Efficiency. *ACS Sustain. Chem. Eng.* **2022**, *10*, 3787–3798. [CrossRef]
33. Cai, C.; Liu, Z.; Li, F.; Yang, Z. Upgrading Cotton-Based Resources for Regenerated Cellulose Fibers, Functional Fibers, Smart Textiles, and Other High-Value Uses. *Carbohydr. Polym.* **2025**, *368*, 124195. [CrossRef] [PubMed]
34. Sáez, R.; McArdle, C.; Salhi, F.; Marquet, J.; Sebastián, R.M. Controlled Living Anionic Polymerization of Cyanoacrylates by Frustrated Lewis Pair Based Initiators. *Chem. Sci.* **2019**, *10*, 3295–3299. [CrossRef] [PubMed]
35. Mwaikambo, L.Y.; Ansell, M.P. Chemical Modification of Hemp, Sisal, Jute, and Kapok Fibers by Alkalization. *J. Appl. Polym. Sci.* **2002**, *84*, 2222–2234. [CrossRef]
36. Peng, H.-Y.; Yeh, K.-Y.; Liu, B.-Y.; Chen, L.-J. Defining Hydrophilicity and Hydrophobicity Through Advancing Contact Angles and Wetting Transitions. *J. Colloid Interface Sci.* **2026**, *708*, 139801. [CrossRef] [PubMed]
37. Cassie, A.B.D.; Baxter, S. Wettability of Porous Surfaces. *Trans. Faraday Soc.* **1944**, *40*, 546–551. [CrossRef]
38. Chen, C.; Li, B.; Wang, Y.; Bian, M.; Kang, X.; Yang, X. Recent Advances on Aluminum-Based Boron Carbide Composites: Performance, Fabrication, and Applications. *Materials* **2025**, *18*, 5469. [CrossRef] [PubMed]
39. Domnich, V.; Reynaud, S.; Haber, R.A.; Chhowalla, M. Boron Carbide: Structure, Properties, and Stability Under Stress. *J. Am. Ceram. Soc.* **2011**, *94*, 3605–3628. [CrossRef]
40. Mondal, S.; Bykova, E.; Dey, S.; Ali, S.I.; Dubrovinskaia, N.; Dubrovinsky, L.; Parakhonskiy, G.; van Smaalen, S. Disorder and Defects Are Not Intrinsic to Boron Carbide. *Sci. Rep.* **2016**, *6*, 19330. [CrossRef] [PubMed]
41. Nurazzi, N.M.; Asyraf, M.R.; Fatimah Athiyah, S.; Shazleen, S.S.; Rafiqah, S.A.; Harussani, M.M.; Kamarudin, S.H.; Razman, M.R.; Rahmah, M.; Zainudin, E.S.; et al. A Review on Mechanical Performance of Hybrid Natural Fiber Polymer Composites for Structural Applications. *Polymers* **2021**, *13*, 2170. [CrossRef] [PubMed]
42. Thévenot, F. State of the Art Boron Carbide: A Comprehensive Review. *J. Eur. Ceram. Soc.* **1990**, *6*, 205–225.
43. Amor, N.; Noman, M.T.; Petru, M. Classification of Textile Polymer Composites: Recent Trends and Challenges. *Polymers* **2021**, *13*, 2592. [CrossRef] [PubMed]
44. Berk Ertekin, G.; Marmaralı, A. Mechanical Properties of Cotton and High-Performance Fiber Blended Denim Fabrics for Motorcycle Protective Clothing. *J. Test. Eval.* **2024**, *52*, 2206. [CrossRef]
45. Xu, S.-A. Effects of Methoxy Polyethylene Glycol–Polycaprolactone Block Copolymers and Silica Nanoparticles on the Mechanical, Tissue Affinity and Antibacterial Properties of n-Butyl Cyanoacrylate Adhesive. *J. Appl. Polym. Sci.* **2023**, *140*, e54342. [CrossRef]
46. *EN 1621-1:2012*; Motorcyclists' Protective Clothing Against Mechanical Impact—Part 1: Limb Joint Impact Protectors. CEN: Brussels, Belgium, 2012.
47. *EN 1621-2:2014*; Motorcyclists' Protective Clothing Against Mechanical Impact—Part 2: Motorcyclists' Back Protectors. CEN: Brussels, Belgium, 2014.
48. *ANSI/ISEA 138-2019*; American National Standard for Performance and Classification for Impact-Resistant Gloves. ISEA: Arlington, VA, USA, 2019.
49. Sharma, S.K.; Sharma, L.K.; Pradhan, R.; Sharma, Y.; Sharma, M.; Gajević, S.; Ivanović, L.; Stojanović, B. Interphase-Centric and Mechanism-Driven Advances in Polymer Composites Reinforced with Nano-, Synthetic, and Inorganic Fillers. *Polymers* **2026**, *18*, 323. [CrossRef] [PubMed]
50. Arora, N.; Dua, S.; Singh, V.K.; Singh, S.K.; Senthilkumar, T. A Comprehensive Review on Fillers and Mechanical Properties of 3D Printed Polymer Composites. *Mater. Today Commun.* **2024**, *40*, 109617. [CrossRef]
51. Kuan, H.T.N.; Tan, M.Y.; Shen, Y.; Yahya, M.Y. Mechanical Properties of Particulate Organic Natural Filler-Reinforced Polymer Composite: A Review. *Compos. Adv. Mater.* **2021**, *30*, 26349833211007502. [CrossRef]
52. Ma, Y.; Wang, J.; Zhao, G.; Liu, Y. New Insights into the Damage Assessment and Energy Dissipation Weight Mechanisms of Ceramic/Fiber Laminated Composites under Ballistic Impact. *Ceram. Int.* **2023**, *49*, 21966–21977. [CrossRef]
53. Lee, J.T.; Kim, M.W.; Song, Y.S.; Kang, T.J.; Youn, J.R. Mechanical Properties of Denim Fabric Reinforced Poly(lactic acid). *Fibers Polym.* **2010**, *11*, 60–66. [CrossRef]
54. Mandal, A.; Habib, A.; Paul, B.; Islam, M.; Ahamed, B.; Islam, S. Integration of recycled denim waste cotton fibre and jute fibre in thermoplastic bio composite applications. *Results Mater.* **2024**, *23*, 100611. [CrossRef]

Disclaimer/Publisher's Note: The statements, opinions and data contained in all publications are solely those of the individual author(s) and contributor(s) and not of MDPI and/or the editor(s). MDPI and/or the editor(s) disclaim responsibility for any injury to people or property resulting from any ideas, methods, instructions or products referred to in the content.